

COMPARING THE ELASTIC CONSTANTS OF POROUS TITANIUM COMPACTS WITH THEORETICALLY PREDICTED VALUES

Ali M. S. Al-Amri

Associate Professor, Department of Agricultural Engineering
King Faisal University, Al-Ahsa 31982, Saudi Arabia

ABSTRACT

Some elastic properties of green and sintered titanium compacts were experimentally measured. The results were compared with the theoretical predictions based on Mackenzie's and Walton's models. It was concluded that the results obtained with the titanium compacts in the present work span a range of behaviour such that no one, simple model can account for the complete range.

NOMENCLATURE

- a : Average radius of contacts.
- n : Average number of contacts between a spherical grain and its neighbours.
- κ : Bulk modulus of the solid material.
- κ^* : Bulk modulus of the titanium compact.
- R : Average radius of a spherical grain.
- ρ : Density of the titanium compact.
- ρ_s : Density of the solid material.
- μ : Shear modulus of the solid material.
- μ^* : Shear modulus of the titanium compact.

INTRODUCTION

The problem of calculating the moduli of porous solids, in general, is one which has been examined by various workers over a number of years [1-12]. Essentially, the problem is formulated in the following way. Given grains of a solid material (assumed isotropic) with known elastic moduli (μ, κ), we wish to calculate

the moduli (μ^*, κ^*) of a collection of grains which are held together by bonding along limited sections of the surface areas of the grains. The simplest approach is to assume that the porosity consists of isolated spherical holes in the solid material. However, the isolated hole model probably does not correspond to some of the structures produced in the present work at high porosities. In this case a better model might consist of spheres bonded together along parts of their circumference. Most theories for the stiffness values of porous materials have been developed for dense bodies with either isolated porosity by Mackenzie [1] or isolated penny-shaped cracks by Walsh [3], both of which are distributed randomly. These theories were originally restricted to low concentrations of the pores or cracks which might be a reasonable assumption for the sintered material. The unsintered material though might be different on a microstructure level. Metallographic examination of the sections of unsintered titanium compact presented ambiguous evidence to support this idea. Therefore, the Walton's model [9] for the elastic modulus of weakly bonded spheres connected together by pressure and elastic deformation in a random arrangement was also considered to be a reasonable assumption to interpret the present results of unsintered titanium compacts.

MATERIALS AND METHODS

Sponge titanium powder ($< 100 \mu\text{m}$ in diameter) was used in the present investigation. The powder was cold pressed at various pressures up to 300MPa. The moulded compact (green body) was placed in a rubber bag which was partially evacuated with a vacuum pump. It was then further consolidated by cold isostatic pressing in a Laboratory Isostatic Press. Some specimens were sintered at temperatures between 900 and 1000°C for 5 hours in an atmosphere of flowing argon.

The mechanical properties, such as Young's modulus and Poisson's ratio, were measured using four-point bend loading in which the specimen strain was measured directly by strain gauges cemented to the specimen surface. By measuring the bending deflection of the test specimen, it was possible to calculate the Young's modulus using a simple theory by Stephens [13]. In the results described below, the measured values of Young's modulus, E , and Poisson's ratio, ν , were used to calculate the shear modulus μ and bulk modulus κ using the isotropic approximation [14]. These two quantities are more fundamental since they represent the resistance to shape change and volume change, respectively. The relations between these parameters are :-

$$\mu = \frac{E}{2(1 + \nu)} \quad (1)$$

$$\kappa = \frac{E}{3(1 - 2\nu)} \quad (2)$$

(The percentages of errors involved in using equations (1) and (2) with solid titanium values against experimental values for compact titanium were 12% for equation (1) and 15% for equation (2))

The density and porosity were determined by the standard water displacement method described by Prokic [15].

RESULTS AND DISCUSSION

The results were formulated and expressed by the above two models i.e. Walton's model [9] for a collection of grains similar to the structures shown in Fig. 1 and Mackenzie's model [1] for the isolated holes in a solid material as depicted in Fig. 2. It can be shown that Walton's model gives the following results when interpreted in terms suited to the present discussion, the shear modulus of the compact is given by

$$\mu^* = \frac{0.8}{\pi} C n \frac{a \rho}{R \rho_s} \mu \quad (3)$$

where n is the average number of contacts between a spherical grain and its neighbours. It is expected that n takes a value between 4 and 6. Taking $n = 5$ as an average value we have :

$$\frac{\mu^*}{\mu} = \frac{4}{\pi} C \frac{a \rho}{R \rho_s} \quad (4)$$

$$\text{where } C = \frac{(1 + \mu/\kappa) (1 + \frac{1}{3} \mu/\kappa)}{(1 + \frac{2}{3} \mu/\kappa) (1 + \frac{4}{3} \mu/\kappa)} \quad (\text{see Appendix - A}) \quad (5)$$

and a is the average radius of contact, and R is the average radius of a spherical grain (see Figs 3 and 4). The ratio a/R is likely to be between 0 and 0.3 depending on the bonding between the grains. ρ is the density of the compact and ρ_s is the density of the solid material.

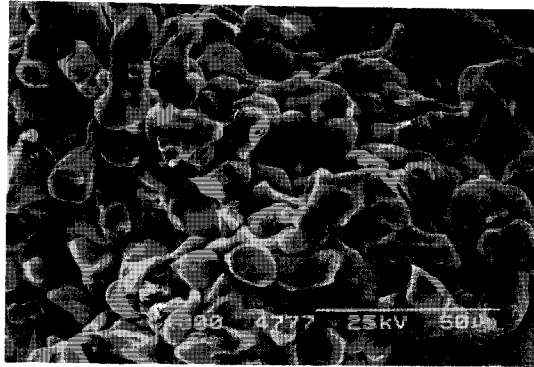


Fig. 1. Fracture surface of unsintered titanium compacts, bonded at high compaction pressure (300MPa), Young's Modulus (34GPa)

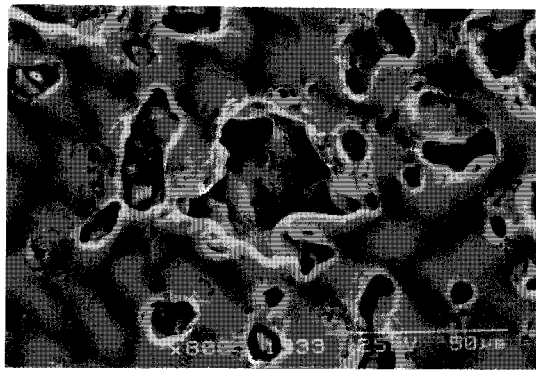


Fig. 2. Isolated holes in the titanium compacts (sintered for 5 hrs at 900°C, compacted at 300 MPa)

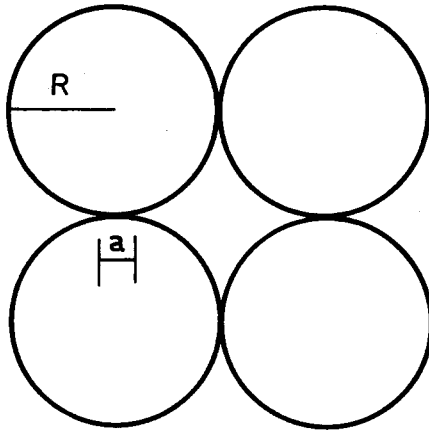


Fig. 3. Random arrangement of weakly bonded spheres as used in Walton's model [9]



Fig. 4. Fracture surface of unsintered titanium compacts, grains (or particles) are bonded along parts of their circumference (140MPa compaction pressure) similar to the random spheres of Walton's model

A plot of μ^*/μ versus the porosity $(1-\rho/\rho_s)$ is shown in Fig. 5 for selected values of a/R between 0 and 0.3. It is clear that the shear modulus of the compact is strongly influenced by the radius of the bonding area a between the grains in Fig. 5 (Walton's model).

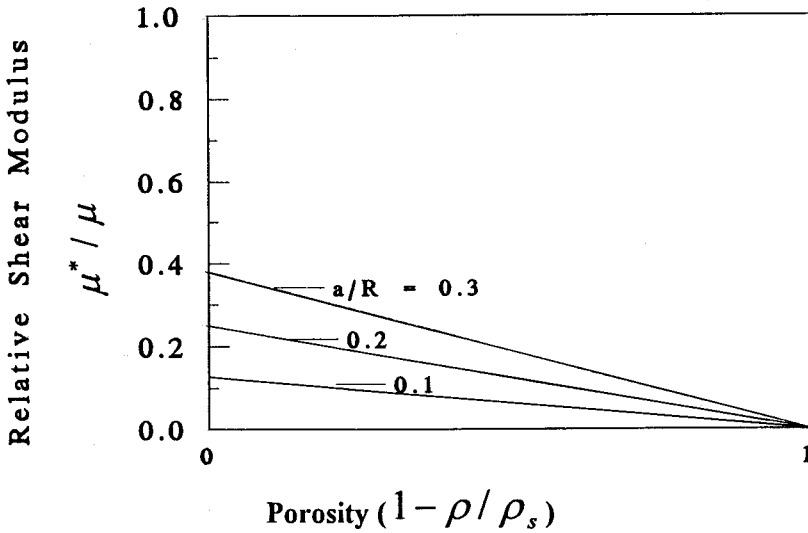


Fig. 5. Relative shear modulus μ^*/μ versus the porosity for some values of a/R between 0 and 0.3 in Walton's model

Walton's model also gives the ratio of the shear modulus μ^* to bulk modulus κ^* of the compact. It turns out that the ratio is independent of the porosity and the contact radius, i.e.

$$\frac{\mu^*}{\kappa^*} = 1.2 \frac{\left[1 + \frac{\mu}{\kappa}\right]}{\left[1 + \frac{2\mu}{3\kappa}\right]} \quad (\text{see Appendix - A}) \quad (6)$$

where μ and κ are the shear and bulk moduli of the solid material, respectively. For solid titanium $\mu/\kappa = 0.3$ as is, typical of many soft metals. Inserting this value in equation (6) above gives $\mu^*/\kappa^* = 1.3$, i.e. Walton's model predicts a high ratio of shear to bulk modulus.

We now consider Mackenzie's model of a porous solid which was formulated on the basis that the pores are isolated (Fig. 2). In fact, Mackenzie assumed that the porous material contains spherical voids which do not interact strongly with one another. For the shear modulus Mackenzie obtained,

$$\frac{\mu^*}{\mu} = 1 - \frac{5}{8} \left[\frac{\left\{ \frac{3}{8} + \frac{1}{2} \frac{\mu}{\kappa} \right\}}{\left\{ \frac{9}{8} + \frac{\mu}{\kappa} \right\}} \left\{ 1 - \frac{\rho}{\rho_s} \right\} \right] \quad (7)$$

and for the ratio of shear to bulk modulus,

$$\frac{\mu^*}{\kappa^*} = \left[1 - \frac{5}{8} \frac{\left\{ \frac{3}{8} + \frac{1}{2} \frac{\mu}{\kappa} \right\}}{\left\{ \frac{9}{8} + \frac{\mu}{\kappa} \right\}} \left\{ 1 - \frac{\rho}{\rho_s} \right\} \right] \left[\frac{\frac{\mu}{\kappa} \frac{\rho_s}{\rho} + 3 \left\{ 1 - \frac{\rho}{\rho_s} \right\}}{\frac{\rho}{\rho_s}} \right] \quad (8)$$

Inspection of equation (7) shows that Mackenzie's expression for the shear modulus may not be correct for very porous solids because it fails to reach the limit $\mu^*/\mu \rightarrow 0$ as $\rho/\rho_s \rightarrow 0$. Thus we must take Mackenzie's result for the shear modulus to be appropriate only in the limit of dilute porosity. However, the interesting feature of Mackenzie's model is that in contrast to the shear modulus, the bulk modulus falls rapidly as the porosity increases. This is very roughly in line with our experience of the behaviour of the titanium compacts where the bulk modulus falls more rapidly with porosity than the shear modulus (see Fig. 6). There is an analogy here with the behaviour of liquids containing small bubbles of gas. It is known that the bulk modulus of liquids containing gas can be very much lower than that of the de-gassed liquid. In contrast the viscosity of the liquid (resistance to shape change) is relatively little affected by the gas content.

The experimental results for the titanium compacts are compared with the various theoretical predictions in Figs 7 and 8. Figure 7 shows the shear modulus ratio μ^*/μ as a function of porosity $(1 - \rho/\rho_s)$. Clearly the moduli are much lower than what Mackenzie's model predicts. Walton's model gives some results closer within the range of observed values, but, of course the relation is adjustable depending on the value of the contact radius a chosen. From this it is possible to interpret the experimental results as showing values of a/R for the titanium compacts which are not independent, but vary with the porosity.

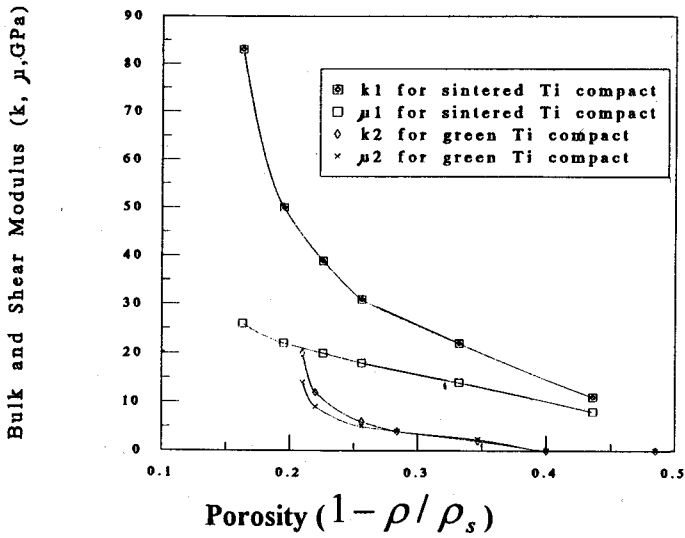


Fig. 6. K and μ as a function of porosity for sintered and green titanium compacts

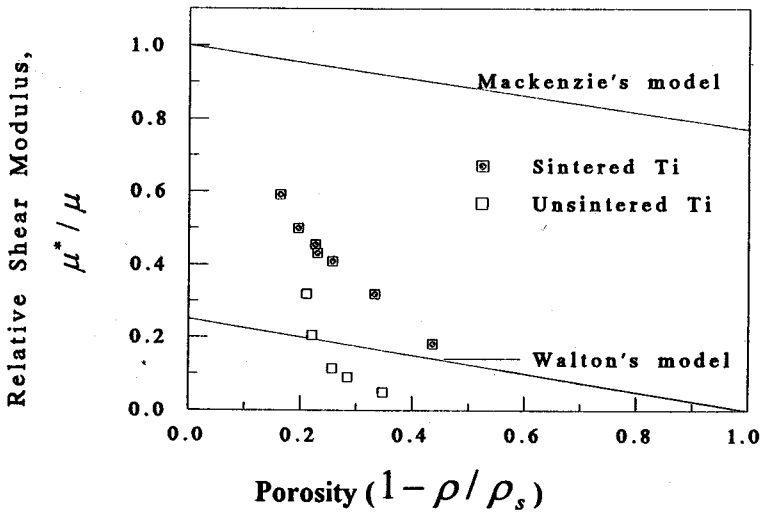


Fig. 7. Comparison of the experimental results with the models of Walton at ($a/R = 0.2$) and Mackenzie

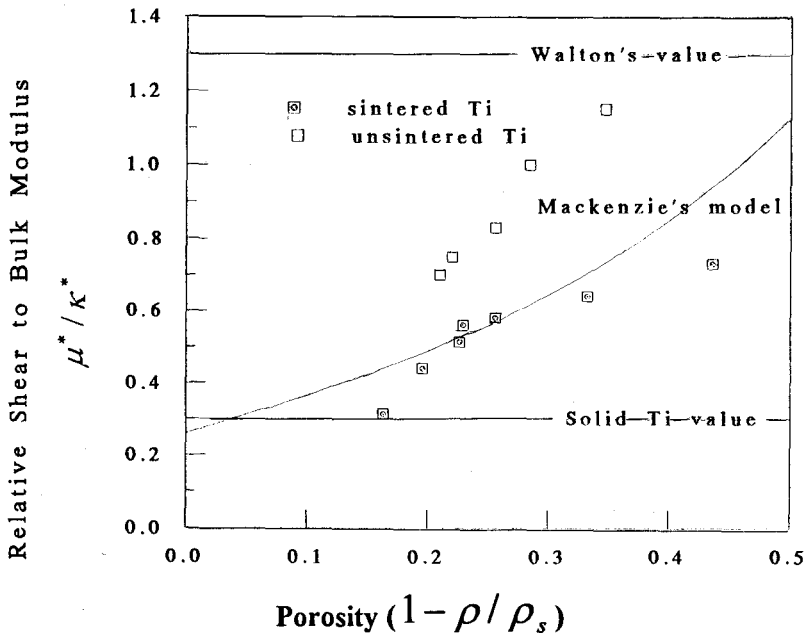


Fig. 8. Experimental results of the relative shear to bulk modulus of sintered and unsintered titanium compacts compared with Mackenzie's [1] model, the value of Walton's[9] model and with the solid titanium value

The problem in understanding the moduli values of porous solids is that a wide range of behaviour can occur, depending on the model adopted. The results we have obtained with the titanium compacts in the present work probably span a range of behaviour such that no one, simple model can account for the complete range. Figure 8 shows that the relation of μ^*/κ^* , for the compacts compressed to the highest pressure and then sintered is probably close in behaviour to the isolated porosity model. At the other extreme, the unsintered compacts found at the lowest pressure are probably quite close to the weakly bonded sphere model.

CONCLUSION

In qualitative terms, the following conclusions can be made:

- 1- In the unsintered compacts, κ^* is small relative to μ^* . One interpretation of this is that the compacts are relatively unresistant to a change in volume compared with the solid material, e.g. that the holes in the structure are opened or closed more easily than the shape of the compact is changed.
- 2- In the sintered compacts, κ^* falls off more rapidly than μ^* as the porosity is increased. Again this indicates a relative reduction in resistance to volume change compared with resistance to shape change.

REFERENCES

1. Mackenzie, J.K., 1950. The Elastic Constants of a Solid Containing Spherical Holes. Proc Phys Soc, London, Vol. B63, No. 1, pp. 2-11.
2. Walsh, J.B., Brace, W.F and England, A.W., 1965. Effect of Porosity on Compressibility of Glass. J. of the Amer Ceram Soc. Vol. 48, No. 12, pp. 605-608.
3. Walsh, J.B., 1965. The Effect of Cracks on the Compressibility of Rocks. J. Geophys Res, Vol. 70, No.2, pp. 381-389.
4. Brace, W.F., 1965. Some New Measurements of Linear Compressibility of Rocks. J. of Geophysical Research. Vol. 70, No. 2, pp. 391-398.
5. DeHoff, R.T., 1965. The Estimation of Particle-Size Distributions from Simple Counting Measurements Made on Random Plane Sections. Transactions of the Metallurgical Society of AIME. Vol. 233, pp. 25-29.
6. Walton, K., 1975. The Effective Elastic Moduli of Model Sediments. Geophys. J. R. Astr. Soc. Vol. 43, pp. 293-306.
7. Walton, K., 1977. Elastic Wave Propagation in Model Sediments-I. Geophys. J. R. Astr. Soc. Vol. 48, pp. 461-478.

8. Digby, P.J., 1981. The Effective Elastic Moduli of Porous Granular Rocks. *J. of Applied Mechanics*. Vol. 48, pp. 803-808.
9. Walton, K., 1987. The Effective Elastic Moduli of a Random Packing of Spheres. *J. Mech Phys Solids*. Vol. 35, No. 2, pp. 213-226.
10. Al-Amri, A and Evans, J.T., 1994. Degradation of the Strength of Glass After Light Contact With Other Materials. *J. Materials Science and Engineering*, Vol. A177, pp. 11-18.
11. Chapman, A.M and Higdon, J.J.L., 1994. Effective Elastic Properties for a Periodic Biocontinuous Porous Medium. *J. Mech. Phys. Solids*. Vol. 42, No. 2, pp. 283-305.
12. Al-Amri, A.M.S., 1997. Mechanisms of Contact Damage to High Strength Containers by Handling Materials. *Sudan Eng. Soc. J.*, Vol. 44. No. 34. pp. 47-54.
13. Stephens, R.C., 1975. *Strength of Materials, Theory and Examples*. Edward Arnold Ltd., London.
14. Young, W.C., 1989. *Roark's Formulas for Stress and Strain*, 6th edition. McGraw-Hill Book Co., New York.
15. Prokic, D., 1974. The Application of Modern Single-Pan Analytical and Microanalytical Balances to Measurements of the Densities of Solids. *J. Phys D: Appl Phys*. Vol. 7, pp. 1873-1876.

APPENDIX - A

This Appendix interprets Walton's (1987) model in to terms appropriate for unsintered titanium compact materials as follows:

$$B = \frac{1}{4\pi} \left\{ \frac{1}{\mu} + \frac{1}{\mu + \lambda} \right\} = \frac{1}{4\pi} \times \frac{2\mu + \lambda}{\mu(\mu + \lambda)}; \quad C = \frac{1}{4\pi} \left\{ \frac{1}{\mu} - \frac{1}{\mu + \lambda} \right\} \quad (\text{A.1})$$

$$\frac{5B + C}{2B + C} = 2 \frac{3\mu + 3\kappa}{2\mu + 3\kappa} = 2 \frac{1 + \mu/\kappa}{1 + \frac{2\mu}{3\kappa}} \quad (\text{A.2})$$

$$\mu^* = \frac{1}{10} \times \frac{5B + C}{2B + C} \left[\frac{3\phi^2 n^2 p}{\pi^4 B^2} \right]^{1/3} \quad (\text{A.3})$$

$$\kappa^* = \frac{1}{6} \left[\frac{3\phi^2 n^2 p}{\pi^4 B^2} \right]^{1/3} \quad (\text{A.4})$$

$$\text{Hence,} \quad \frac{\mu^*}{\kappa^*} = \frac{6}{5} \frac{\left[1 + \frac{\mu}{\kappa} \right]}{\left[1 + \frac{2\mu}{3\kappa} \right]} \quad (\text{A.5})$$

$$\text{Area of contact} \quad a^2 = W_o R \quad (\text{A.6})$$

$$\text{Compacting strain} \quad e = \frac{W_o}{R} = \left(\frac{a}{R} \right)^2 \quad (\text{A.7})$$

$$P = \frac{\phi n}{3\pi^2 B} \left[\frac{a^2}{R^2} \right]^{3/2} = \frac{\phi n}{3\pi^2 B} \left(\frac{a}{R} \right)^3 \quad (\text{A.8})$$

$$\text{Thus} \quad \left[\frac{\phi^2 n^2}{\pi^4 B^2} \times \frac{\phi n}{\pi^2 B} \left(\frac{a}{R} \right)^3 \right]^{1/3} = \frac{\phi n a}{\pi^2 B R} \quad (\text{A.9})$$

$$\text{From equation (A.3)} \quad \mu^* = \frac{0.2}{\pi^2} \frac{(1 + \mu/\kappa)}{(1 + \frac{2}{3}\mu/\kappa)} \frac{\phi na}{B R} \quad (\text{A.10})$$

$$\text{since, } \phi = \frac{\rho}{\rho_s} \quad (\text{A.11})$$

$$\text{Thus } \mu^* = \frac{0.2}{\pi^2} \frac{(1 + \mu/\kappa)}{(1 + \frac{2}{3}\mu/\kappa)} \frac{1 na \rho}{B R \rho_s} \quad (\text{A.12})$$

$$\lambda = \kappa - \frac{2}{3}\mu \quad (\text{A.13})$$

$$2\mu + \lambda = 2\mu + \kappa - \frac{2}{3}\mu = \frac{4}{3}\mu + \kappa \quad (\text{A.14})$$

$$\mu + \lambda = \mu + \kappa - \frac{2}{3}\mu = \frac{1}{3}\mu + \kappa \quad (\text{A.15})$$

Substitute equation (A.15) in to equation (A.1) :

$$B = \frac{1}{4\pi} \frac{\frac{4}{3}\mu + \kappa}{\mu(\frac{1}{3}\mu + \kappa)} = \frac{1}{4\pi} \frac{(1 + \frac{4}{3}\mu/\kappa)}{\mu(1 + \frac{1}{3}\mu/\kappa)} \quad (\text{A.16})$$

$$\mu^* = \frac{0.2}{\pi^2} \frac{(1 + \mu/\kappa)}{(1 + \frac{2}{3}\mu/\kappa)} \frac{4\pi(1 + \frac{1}{3}\mu/\kappa)\mu}{(1 + \frac{4}{3}\mu/\kappa)} \frac{na \rho}{R \rho_s} \quad (\text{A.17})$$

$$\mu^* = \frac{0.8}{\pi} C \frac{\mu na \rho}{R \rho_s} \quad (\text{A.18})$$

$$C = \frac{(1 + \mu/\kappa)}{(1 + \frac{2}{3}\mu/\kappa)} \frac{(1 + \frac{1}{3}\mu/\kappa)}{(1 + \frac{4}{3}\mu/\kappa)} \quad (\text{A.19})$$

$$\text{Poisson's Ratio; } \nu = \frac{\kappa - \frac{2}{3}\mu}{2(\kappa + \frac{1}{3}\mu)} = \frac{1 - \frac{2}{3}\mu/\kappa}{2(1 + \frac{1}{3}\mu/\kappa)} \quad (\text{A.20})$$

$$\text{Thus, } 2\nu(1 + \frac{1}{3}\mu/\kappa) = 1 - \frac{2}{3}\mu/\kappa \quad (\text{A.21})$$

$$\text{and, } 2\nu + \frac{2\mu}{3\kappa}\nu + \frac{2\mu}{3\kappa} = 1; \frac{\mu}{\kappa}(\frac{2}{3}\nu + \frac{2}{3}) = 1 - 2\nu \quad (\text{A.22})$$

$$\therefore \frac{\mu}{\kappa} = \frac{3(1 - 2\nu)}{2(1 + \nu)} \quad (\text{A.23})$$

$$\nu = 0.381 \quad \text{for solid titanium thus, } \frac{\mu}{\kappa} = 0.26 \quad (\text{A.24})$$

$$\therefore C = \frac{1.26}{1.17} \times \frac{1.087}{1.35} = 0.867$$

$$\frac{\mu^*}{\mu} = \frac{0.8}{\pi} C \frac{na}{R} \frac{\rho}{\rho_s} = 0.22 \frac{na}{R} \frac{\rho}{\rho_s} \quad (\text{A.25})$$